Desalination and Water Treatment
www.deswater.com

doi: 10.5004/dwt.2023.29520

295 (2023) 64–72
May

Outstanding adsorption characteristics of an aminophosphonic acid chelating fiber for calcium and magnesium ions

Da-Xin Liu[a], Gang Xu[a,b], Zhao-Wen Chen[c], Guo-Qing Huang[c], Ming-Hong Wu[a,*]

[a]*School of Environmental and Chemical Engineering, Shanghai University, Shanghai 200444, China, emails: mhwu@shu.edu.cn (M.-H. Wu), 1967145467@qq.com (D.-X. Liu), xugang@shu.edu.cn (G. Xu)*
[b]*Key Laboratory of Organic Compound Pollution Control Engineering, Ministry of Education, Shanghai 200444, China*
[c]*Purification Equipment Research Institute of CSIC, Zhanlan Road 1, Handan, 056027, China, emails: 18634101913@163.com (Z.-W. Chen), huang.guoqing1984@163.com (G.-Q. Huang)*

Received 18 September 2022; Accepted 2 April 2023

ABSTRACT

The study focused on the synthesis and applications of an aminophosphonic acid chelating fiber (PAN-PNa) for the deep removal of Ca^{2+} and Mg^{2+} from aqueous solutions in the chlor-alkali industry. As an effective material for the replacement of aminophosphonic acid resins, PAN-PNa achieved outstanding adsorption results for Ca^{2+} and Mg^{2+}. The material was prepared by the Kabachnik-Fields one-pot reaction using an amine-based fiber (PAN-PEI) as precursor. The saturated adsorption capacities of PAN-PNa for Ca^{2+} and Mg^{2+} were significantly higher than those of existing aminophosphonic acid resin, reaching 3.07 and 3.12 mmol/g, respectively. These values were sustained even at low ion concentrations, and in a wide pH range of 3–11 and 3–10, respectively. The adsorption of the ions reached equilibrium within 5 min, which is an excellent improvement from conventional granular adsorbents (about 40–80 min). The excellent performance of PAN-PNa was attributed to its phosphoramidate group and special nano-towed structure. Therefore, by exhibiting both fast adsorption rate and high adsorption capacity at low ion concentration, PAN-PNa is a promising new material for the deep removal of Ca^{2+} and Mg^{2+} from aqueous solutions.

Keywords: Aminophosphonic acid fiber; Calcium; Magnesium; Chlor-alkali; Adsorption

1. Introduction

The removal of Ca^{2+} and Mg^{2+} is critical in the chlor-alkali industry because these ions can cause scaling on the inner walls of tubes, thereby making cleaning difficult, increasing energy consumption, and reducing product quality. The concentration of the ions is key to ensuring the normal operation of ion membrane electrolytic cells in the ion membrane caustic soda project for the chlor-alkali industry. This is because ion concentration affects the service lives of ion membranes, while also being an essential factor for achieving high current efficiencies during operations at high current densities. If the supplied brine to an electrolytic cell contains high concentrations of Ca^{2+} and Mg^{2+} over time, there will be significant decline in the current efficiency, resulting in increased cell voltage, which will ultimately affect the performance of the ion membrane and shorten its service life [1–3]. Therefore, purification (especially the deep purification of Ca^{2+} and Mg^{2+}) is a key process in the chlor-alkali industry. High requirements for the deep removal of Ca^{2+} and Mg^{2+} have been proposed to reduce energy consumption with the intensified competition of chlor-alkali plants [4].

The first fundamental factor for the deep removal of Ca^{2+} and Mg^{2+} is the equilibrium constant of the sorbents. In this regard, the most commonly used sorbents for the deep removal of Ca^{2+} and Mg^{2+} in the chlor-alkali industry are

* Corresponding author.

chelating materials which are special types of ion exchange materials containing functional groups with atoms such as N, O, S, and P, and have lone pairs of electrons that can form coordination bonds with specific metal ions. Therefore, the chelating materials have extremely high equilibrium constants for target ions and can be successfully applied in deep purification [5,6]. According to the chelating groups, the chelating materials are mainly amines [7–11], aminocarboxylic acids [12], mercaptos [13], amidoximes [14–18], aminophosphonic acids [19–34] etc. Among the fiber types, aminophosphonic acid has a stronger binding strength to Ca^{2+} and Mg^{2+}, and its functional group, $–NHCH_2P(O)(OH)_2$, can provide both a chelation center and an ion exchange center.

As adsorption equilibria are usually not reached under the actual working conditions of trace metal ions removal, the adsorption rate is another key factor to be considered for the deep removal of Ca^{2+} and Mg^{2+}. The currently used aminophosphonic acid chelating materials are mainly divided into resins and fibers. While resin materials were reported in the 1960s [35],[5] and patents of mature products appeared in Europe and the United States in the 1980s and 1990s [36,37], fibers are new types of materials developed after resins. Compared with resins, the diameter of a typical fiber is 1–2 orders of magnitude smaller, giving them larger effective contact areas with adsorbents, smaller resistance to fluids, and shorter diffusion channels, allowing the exchange groups to fully react. Therefore, they exhibit high adsorption efficiencies, can deeply purify and adsorb trace substances, and possess obvious kinetic advantages [38–42]. However, the use of aminophosphonic acid fibers in the deep removal of Ca^{2+} and Mg^{2+} has not been reported in the literature, and are yet to be commercialized.

In the light of the above considerations, aminophosphonic acid chelating fiber is possibly a highly efficient Ca^{2+} and Mg^{2+} deep scavenging material that can replace resins. In this study, an amine-based fiber, PAN-PEI [43,44], was used as a matrix to prepare aminophosphonic acid fibers through Kabachnik-Fields reaction, and its ability to adsorb Ca^{2+} and Mg^{2+} in aqueous solution was examined. The outcome of this investigation is expected to be of great interest to the chlor-alkali industry as there is a growing search for effective and efficient methods for the purification of Ca^{2+} and Mg^{2+}.

2. Experiments

2.1. Materials and methods

All reagents were used as received. Formaldehyde (AR), concentrated hydrochloric acid (AR) and sodium hydroxide (AR) were purchased from Tianjin Ou Boke Chemical Reagent Products Sales Co., Ltd., Tianjin, China. Phosphorous acid (AR) was purchased from Shanghai Macklin Biochemical Co., Ltd., Shanghai, China. The 1,8-diazabicyclo[5.4.0] undec-7-ene (DBU) used in this study was purchased from Shandong Xinhua Wanbo Chemical Industry Co., Ltd., Shandong, China. PEI (98% purity, relative molecular weight of 1800) was supplied by Gongbike New Material Technology (Shanghai) Co., Ltd., Shanghai, China, and PAN fibers with linear density of 1.67 dtex were supplied by Acrylic Factory of Qilu Branch of Sinopec, Shandong, China.

2.2. Preparation of amine fiber PAN-PEI

The preparation of PAN-PEI followed the procedures outlined in our previous studies [43,44]. In the typical experiment, 4 g PAN fiber and 400 mL 8% DBU aqueous solution were added into a 500 mL flask, and refluxed at 100°C (boiling) for 4 h. Then the fibers were immersed into 1 mol/L hydrochloric acid solution for 2 h. After that, the fibers were taken out and washed with deionized water to neutral conditions to obtain PAN-COOH fibers. 4 g PAN-COOH fibers and 400 mL 1% PEI aqueous solution were added together into a 500 mL flask, and the solution was refluxed at 100°C (boiling) for 1 h. After the reaction was completed, the fibers were taken out and washed with deionized water to neutral conditions to obtain crosslinked PAN fibers (PEI-PAN). 4 g PEI-PAN fiber and 400 mL 0.5 wt.% sodium hydroxide aqueous solution were added into a 500 mL flask, and the solution was refluxed at 100°C (boiling) for 2.5 h. After the reaction, the fibers were taken out and immersed into 1 mol/L hydrochloric acid solution for 5 h. After that, the fibers were taken out and washed to neutral conditions to obtain crosslinked PAN-COOH fiber (PEI-PAN-COOH). 4 g PEI-PAN-COOH fiber and 400 mL 10 wt.% PEI aqueous solution were added into a 500 mL flask, and the solution was refluxed at 100°C (boiling) for 2 h. After the reaction, the fibers were taken out and washed with deionized water to neutral conditions to obtain PAN-PEI fibers.

2.3. Preparation of aminophosphonic acid chelating fiber PAN-PNa

Through orthogonal experiments, optimal parameters such as reaction temperature, reaction time, HCl concentration, and material ratio were selected, and the following materials used in this investigation were prepared under optimal conditions.

97 mL distilled water and 203 mL concentrated hydrochloric acid were added into a beaker, followed by 12.5 g phosphorous acid. The solution was transferred into a 500 mL three-necked flask after complete dissolution. 3 g PAN-PEI fibers (with total amine groups amount of 5.8 mmol/g) was immersed into the solution and preheated to 65°C. Then 12.3 mL formaldehyde was added into the flask under shaking, and the temperature was adjusted to keep the solution slightly boiling for 9 h. The fibers were taken out after complete reaction and washed 5 times with deionized water to afford the PAN-PH fibers. The PAN-PH fibers were immersed into 1 N NaOH solution, and shaken for 5 min. Then the fibers were taken out and washed with deionized water to neutral, and air-dried at room temperature to obtain the sodium aminophosphonate-type fiber (PAN-PNa). The reaction scheme is outlined in Fig. 1.

2.4. Characterization

2.4.1. Elemental analysis (EA)

C, H, N, S, O elements were analyzed by Vario EL cube method; The element P was analyzed by an Agilent inductively coupled plasma emission spectrometer (Agilent ICPOES730 instrument).

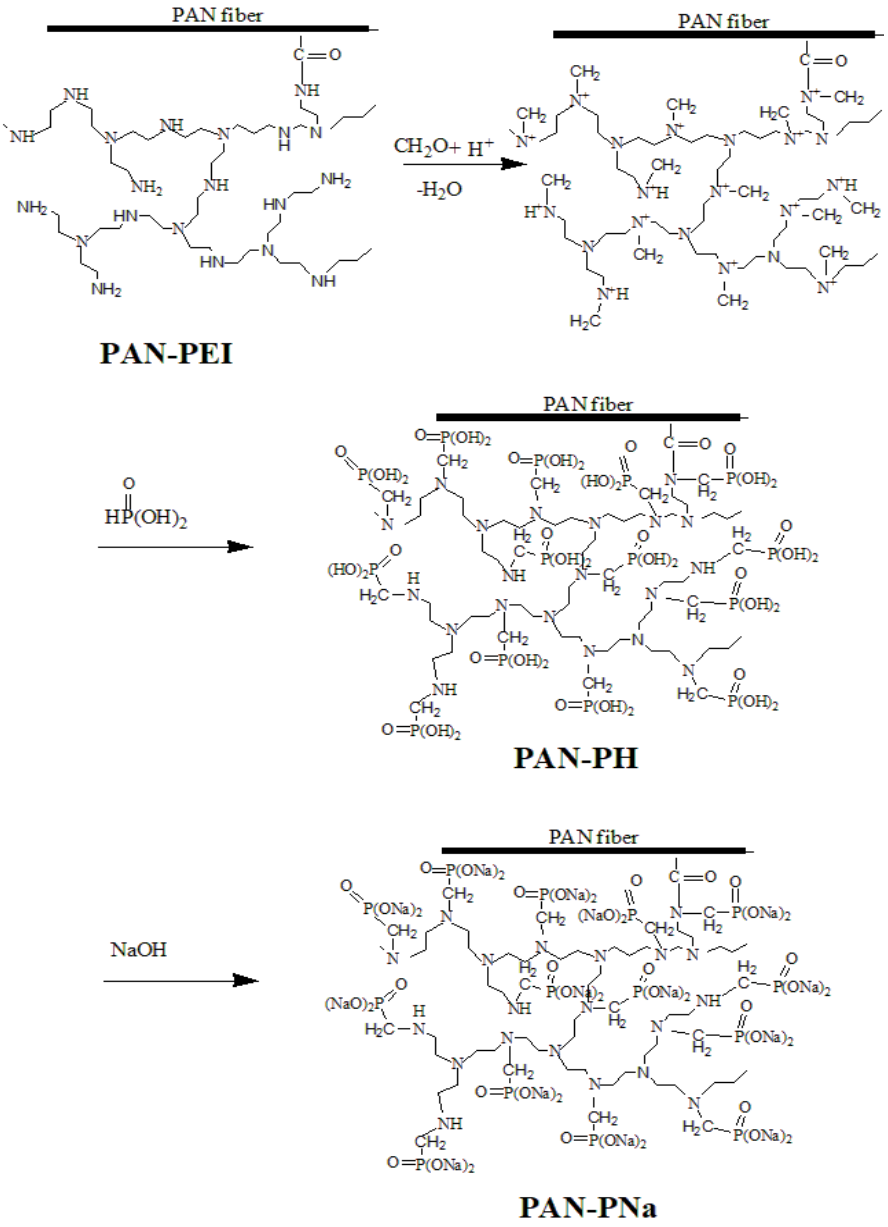

Fig. 1. Schematic diagram of the reactions pathway from PAN-PEI to PAN-PNa.

2.4.2. Fourier-transform infrared spectroscopy

Fourier transform infrared spectroscopy analysis was performed on the PAN-PEI, PAN-PH, PAN-PNa, and phosphorous acid. Each test sample was placed in a mortar with KBr in a weight ratio of 1:100, fully grounded and pressed into tablets for analysis by Fourier-transform infrared spectroscopy (FTIR, Spectrum Two, manufactured by PerkinElmer, USA) at the range of 4,000–500 cm^{-1}.

2.4.3. Nuclear magnetic resonance spectroscopy

The ^{31}P NMR tests were performed on a JNM-ECZ600R NMR spectrometer at a resonance frequency of 242.95 MHz. The spectra were recorded at a spinning rate of 15 kHz with a 3.2 mm probe at room temperature. All the tests were performed with a delay time of 5 s.

2.4.4. Scanning electron microscopy and energy-dispersive X-ray spectroscopy

Scanning electron microscopy (SEM) and energy-dispersive X-ray spectroscopy (EDS) analysis were performed on the fibers using the instrument: Hitachi SU8010 Cold Field Emission SEM, Sedona SD Detector (Model: SDD3030-300C+). Prior to the surface morphology analysis, the fibers were pasted on a conductive adhesive and gold-sputtered. For the cross-sectional morphology scanning, the fiber samples were embedded in a hot-melt adhesive, and then cut into several slices with a blade. Slices with good shapes were

carefully separated and cut into 1 mm thick slices. These slices were then pasted on the conductive adhesive and gold-sputtered.

2.4.5. Adsorption test for Ca^{2+} and Mg^{2+}

2.4.5.1. Adsorption rate test

$CaCl_2$ and $MgCl{\cdot}6H_2O$ were used to prepare the metal ion solutions. The initial ion concentration of both Ca^{2+} and Mg^{2+} was 400 mg/L. 0.6 g prepared fibers were immersed into 200 mL Ca^{2+} or Mg^{2+} aqueous solution under shaking, and samples were drawn at regular intervals. The concentration of the metal ions in the water phase was measured using an inductively coupled plasma atomic emission spectrometer ICP Spectrometer (ICAP 7000 Series, Thermo Scientific). The amount of metal ion adsorption was calculated by Eq. (1), where Q is the chelation adsorption capacity (mmol/g), C_0 is the concentration of Ca^{2+}/Mg^{2+} before adsorption (mg/L), C_e is the concentration of Ca^{2+}/Mg^{2+} after adsorption (mg/L), V is the solution volume (L), M is the molar mass of Ca/Mg (g/mol), and m is the fiber mass (g).

$$Q = \left(C_0 - C_e\right) \times V \times \frac{1}{mM}$$

2.4.5.2. Isothermal adsorption capacity test

The adsorption isotherms of the PAN-PNa fiber for Ca^{2+} and Mg^{2+} were determined under the following conditions: The initial Ca^{2+} concentration range was 80–500 mg/L, and the initial Mg^{2+} concentration range was 70–400 mg/L. 0.60 g of the fiber samples were equilibrated with 200 mL of the different concentrations of metal ion solutions at 25°C for 2 h. The equilibrium pH values of the Ca^{2+} and Mg^{2+} solutions were both controlled at 5.5.

2.4.5.3. Test of the influence of pH on adsorption

In this case, the experimental conditions were as follows: 0.60 g of the PAN-PNa fiber was equilibrated in 200 mL of 400 mg/L solution of each metal ion at 25°C for 2 h. The tested pH ranges were 1.0–11.0 for Ca^{2+}, and 1.0–10.0 for Mg^{2+}.

3. Results and discussion

3.1. Characterization studies

Elemental analyses of PAN, PAN-PEI, and PAN-PNa fibers were performed to verify the success of the phosphorylation and accurately determine the content of the phosphate groups. Table 1 shows the weight ratios of C, H, O, N, P, and S in PAN-PEI and PAN-PNa. The proportion of P element changed from almost zero in PAN to 4.88 in PAN-PNa after the phosphonation process, indicating the successful introduction of P-containing functional groups. In addition, the increase of C/N ratio and the decrease of C/O ratio also validates the alkylation and phosphorylation reaction process.

EDS analysis was performed to further characterize the distribution of functional groups on the surface of the fibers and the results are displayed in Fig. 2. The analysis showed significant distribution of P element on the surface of the fibers. Also, the contents of N, O, and P measured using EDS were significantly higher than those listed in Table 1, indicating that the effective functional groups showed a certain aggregation on the surface of the fiber.

To analyze the functional groups, FTIR analysis was conducted and the results are displayed in Fig. 3. The figure represents an infrared comparison chart of P (phosphorous acid reagent), PAN-PEI, PAN-PH (H-type PAN-P), and PAN-PNa (Na-type PAN-P). By comparison, it was found that the P-OH stretching peak appeared at 1,015 cm^{-1} in the phosphite reagent, but splited into two peaks at 1,041 and 911 cm^{-1} upon the conversion of PAN-PEI to PAN-PH. This is because when PAN-PH was converted to sodium-type PAN-PNa, the P-OH became P-ONa. At the same time, the split double peaks shifted towards higher wave numbers, appearing at 1,089 and 969 cm^{-1}, respectively. The analysis also supports the phosphonation process. Furthermore, nuclear magnetic resonance (NMR) analysis was employed to analyze the different types of groups, and the results are shown in Fig. 4. The figure clearly shows that there was no peak on the ^{31}P spectra of PAN-PEI (Fig. 4a), while the ^{31}P NMR spectra of PAN-PNa exhibited double peaks at 17.458 and 9.228, which correspond to the substitutions of $PO(ONa)_2$ on the primary and secondary amines, respectively. This also validates the successful conversion of PAN-PEI to PAN-PNa.

3.2. Characterization of the fiber structure

The fibers were characterized by SEM and EDS mapping as shown in Fig. 5, and the cross-sectional structure of PAN-PEI exhibited a dumbbell shape (Fig. 5a) with a size of about 10–20 μm. Fig. 5b represents the high-powered cross-sectional morphology of PAN-PEI which shows that the width of the exposed tip next to each other was about 50–70 nm, and these may have been formed by the breaking of the nano-tow inside the fiber. The contour of the nano-tow could be clearly seen at the interface between the interruption

Table 1
Elemental analyses of PAN, PAN-PEI, PAN-PNa fibers

Fiber	Element						Element ratio		
	C	H	N	O	P	S	C/N	C/P	C/O
PAN	66.92	6.05	24.52	3.91	0.01	0.02	2.73	8488	17.1
PAN-PEI	50.34	7.29	19.53	21.96	0.13	0.02	2.58	391	2.29
PAN-PNa	31.71	7.52	10.25	23.53	4.88	0.04	3.09	6.50	1.25

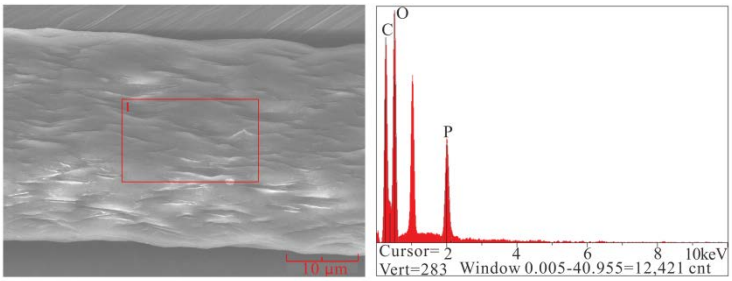

Elt.	Line	Intensity(cis)	Conc	Units	Error2-sig	MDL3-sig	
C	Ka	234.94	29.996	wt.%	0.637	1.712	
N	Ka	46.84	16.254	wt.%	0.897	2.227	
O	Ka	274.70	47.135	wt.%	0.913	2.456	
P	Ka	167.26	6.616	wt.%	0.163	0.420	
			100.000	wt.%			Total

Fig. 2. Field-emission scanning electron microscopy micrographs and energy-dispersive X-ray spectroscopy profile of PAN-PNa fiber.

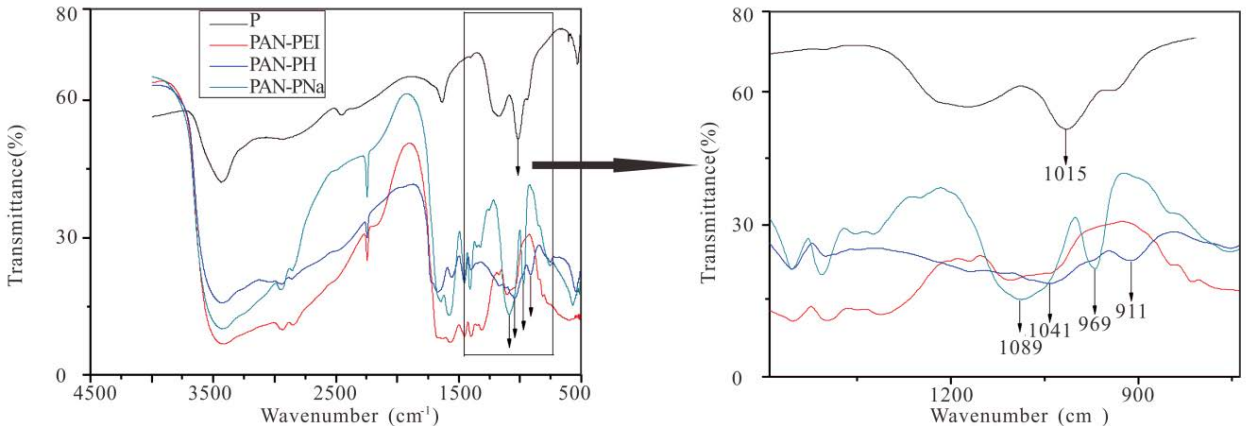

Fig. 3. Fourier-transform infrared spectra and the partially enlarged view of P, PAN-PEI, PAN-PH and PAN-PNa.

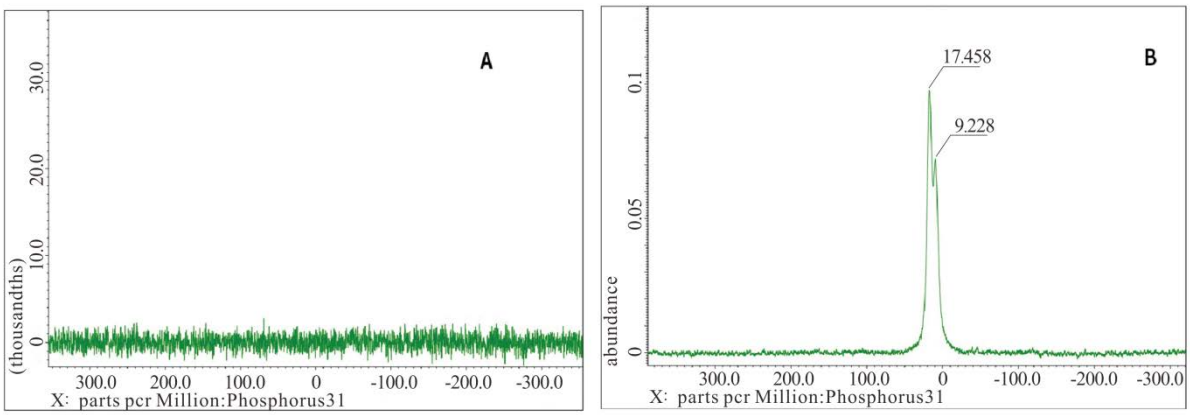

Fig. 4. ^{31}P NMR spectra of (A) PAN-PEI and (B) PAN-PNa fiber.

surface and the surface in Fig. 5b. The surface shown in Fig. 5c had dense grooves with a width of about 20–300 nm. This indicates that the network structure formed by the physical and chemical connections between the nanowire bundles had a network pore size of hundreds of nanometers, and the network pore size may reach micron size when it swells. Figs. 5d and e are SEM images of the cross-section of PAN-PNa, and Fig. 5f depicts its surface morphology.

The network structure of the internal nano-tow was basically the same as that of PAN-PEI. In order to observe the distribution of effective functional groups, a cross-sectional EDS mapping scan was performed on PAN-PNa, and Fig. 5g and h are the P atoms scanning in PAN-PNa, which show even distribution of the P atoms on the cross-section of the fiber, indicating that the aminophosphonic acid functional groups were also distributed on the nano-tow inside the fiber, and not just on the surface of the fiber.

3.3. Calcium and magnesium ion adsorption

Fig. 6 shows the time dependence of the adsorption values of the metal ions on PAN-PNa fibers. As seen in the figure, the initial adsorption rates were very fast at the beginning, followed by a gradual evolution of adsorption equilibrium (plateau values) within 300–500 s for both Ca^{2+} and Mg^{2+}. Its adsorption capacity for Ca^{2+} and Mg^{2+} in the first 20 s was more than 60% of its saturated adsorption capacity. Thus, the adsorption equilibrium was achieved within 5 min, which is a significant improvement from granular adsorbents (with adsorption equilibrium achieved around 40–80 min) [45].

In this investigation, pseudo-first-order and pseudo-second-order reaction kinetic formulas were used for calculations, and the parameters and fitting correlation coefficients are shown in Table 2.

In this reaction, the metal ion reacts in one-to-one contact with the active site on the aminophosphonic acid fiber and is therefore proportional to the product of the remaining active site and the concentration of the metal ion in the solution. Therefore, it is inferred that the chemical reaction obeyed a pseudo-second-order reaction kinetic equation,

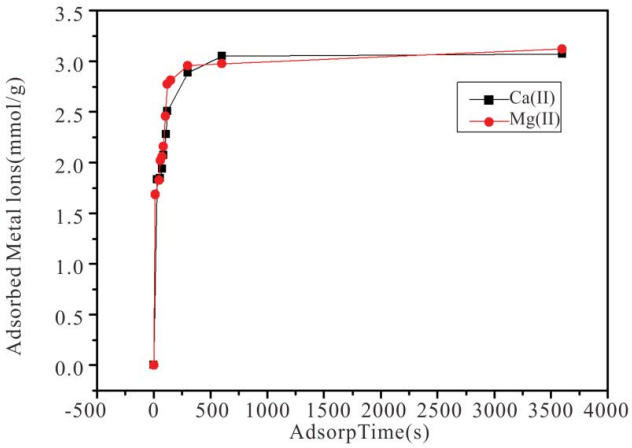

Fig. 6. Adsorption of metal ions by PAN-PNa. Adsorption conditions: initial concentration of metal ions 400 mg/L; pH: 5.5; temperature: 25°C.

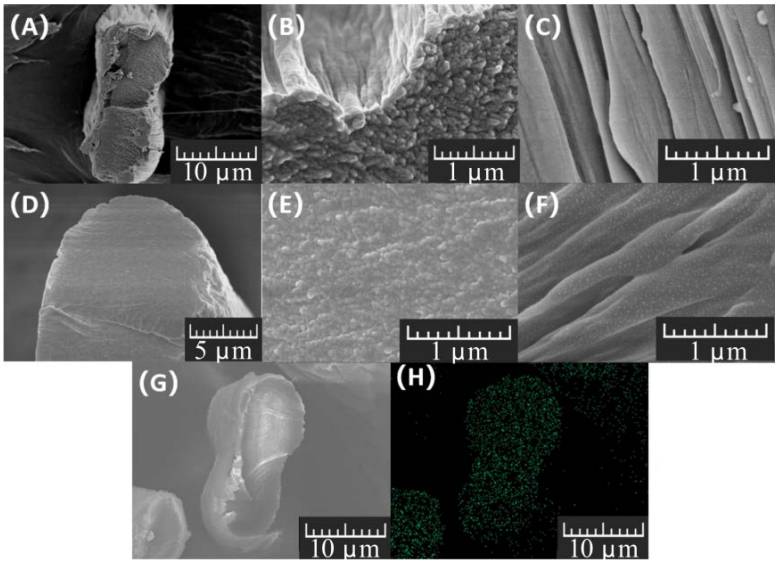

Fig. 5. Cross-sectional SEM micrograph (a,b) and surface SEM micrograph (c) of PAN-PEI fiber; cross-sectional SEM micrograph (d,e) and surface SEM micrograph (f) of PAN-PNa fiber; cross-sectional SEM micrograph (g) and P mapping (h) of PAN-PNa fiber.

Table 2
Kinetic parameters

	Pseudo-first-order fitting parameters			Pseudo-second-order fitting parameters		
	q_e (mmol/g)	k_1 (s^{-1})	R^2	q_e (mmol/g)	k_2 [g·(mmol·s)$^{-1}$]	R^2
Ca^{2+}	2.934	0.0168	0.9080	3.096	0.0116	0.9998
Mg^{2+}	2.916	0.0212	0.8562	3.145	0.0128	0.9998

which is also confirmed by the pseudo-second-order fitting results shown in Table 2.

3.4. Adsorption capacity test

It can be seen from Fig. 7 that the equilibrium adsorption amount of aminophosphonic acid fibers for Ca^{2+} and Mg^{2+} increased with their equilibrium concentrations in solution, and then reached a plateau value, which represents the saturation of the active adsorption sites (that are available for metal ions) on PAN-PNa. The measured saturated adsorption capacities for Ca^{2+} and Mg^{2+} were as high as 3.07 and 3.12 mmol/g, respectively, which are significantly higher than those of existing aminophosphonic acid resins (about 1 mmol/g) [46]. The concentration of Ca^{2+}/Mg^{2+} ions reached saturation at very low concentrations (both below 10 mg/L), indicating the suitability of PAN-PNa fiber for Ca^{2+} and Mg^{2+} adsorption at low concentrations. This also proves that the phosphoramidate group is very suitable for the adsorption of Ca^{2+} and Mg^{2+} at low concentrations.

3.5. Effect of pH on metal binding

As shown in Fig. 8, the adsorption amount of Ca^{2+} was almost 0 when the pH value of the aminophosphonic acid fiber was less than 2, and optimal adsorption amount was attained when the pH reached 3. Moreover, the optimal adsorption amount was maintained in the pH range of 3–11. The pH value was not raised above 11 due to the possibility of precipitation. On the other hand, the adsorption amount of Mg^{2+} was almost 0 at pH < 2 whereas the optimal absorption was attained at pH = 5.83% of the optimal adsorption amount was achieved at pH = 3, and this increased to 93% at pH = 4 until it reached its peak absorption at pH = 5. Subsequently, the absorption amount was maintained in the pH range of 5–10. As with the former, the pH was not raised above 10 due to the presence of precipitates.

Summarily, the aminophosphonic acid fibers did not show adsorption abilities below pH 2, but its optimal adsorptions of Ca^{2+} and Mg^{2+} were maintained in a wide pH range of 3–11 and 3–10, respectively.

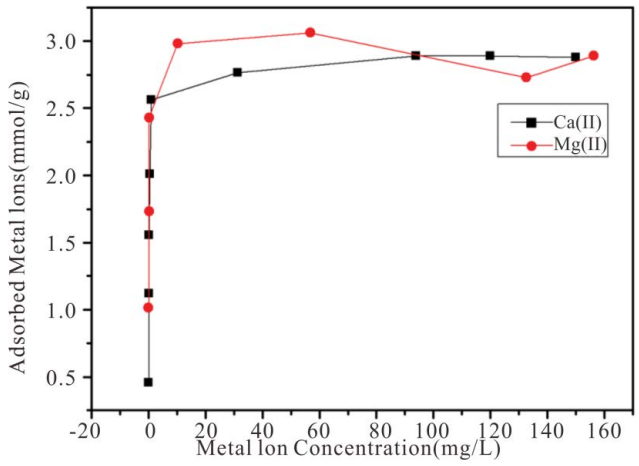

Fig. 7. Adsorption capacity of the PAN-PNa for metal ions. pH: 5.5; temperature: 25°C.

3.6. Analysis of high-speed fiber adsorption mechanism

Compared with other ion exchange fibers, the high-speed adsorption of Ca^{2+} and Mg^{2+} is the biggest advantage of this material. A schematic representative structure of the aminophosphonic acid fiber is presented in Fig. 9 in order to analyze its high-speed adsorption mechanism based on the characterization and analytical results. From the figure, a chelating fiber composed of nano tows and pores is displayed, with the surface of the nano tow being covered with macromolecular amino phosphate groups (the aminophosphonic acid group of the material used was obtained by the phosphonation of polyethyleneimine macromolecules). The size of a tow is about 70 nm, and they are linked to each other through some physical and/or chemical connections, with several hundred nanometers of channels between them (up to the micron level when swelling).

When the Ca^{2+} and Mg^{2+} in solution were exchanged with sodium and amino phosphate ions from the fiber, the whole reaction process went through five stages: First is the membrane diffusion process. The fibers were surrounded by a stationary liquid film, and the ions must pass through the membrane to reach the solid surface. This is called the

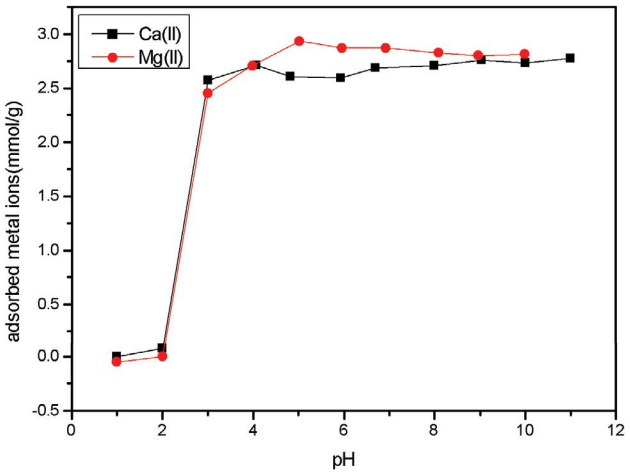

Fig. 8. Effect of pH on adsorption of metal ions on PAN-PNa. Metal ions concentration: 400 mg/L; temperature: 25°C.

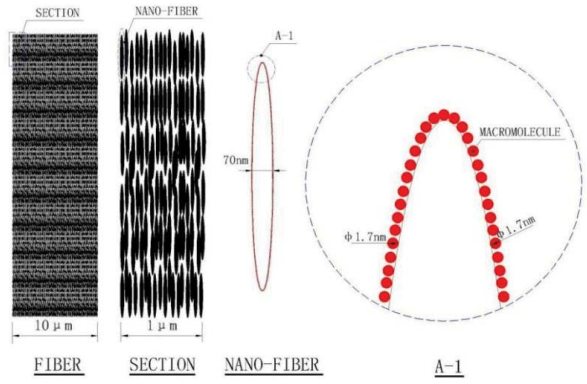

Fig. 9. Schematic representation of the physical structure of PAN-PNa fiber.

membrane diffusion process. Secondly, the Ca^{2+} and Mg^{2+} moved from the surface of the fiber into the interior of the fiber and entered the exchange position. This is the intra diffusion process. Thirdly, the Ca^{2+} and Mg^{2+} are chemically exchanged with sodium ions. Fourthly, the sodium ions travel from the inner part of the fiber to the surface. Finally, the sodium ions were diffused from the surface of the fiber through the liquid membrane and into the external solution.

While steps 1 and 5 are membrane diffusion processes, steps 2 and 4 are inner pore diffusion processes. Due to the high speed of step 3, the whole process is mainly controlled by either the inner pore diffusion or membrane diffusion.

The general coordination adsorption is mainly controlled by the inner pore diffusion. The pore size of the crosslinked gel resin was between 0.5–5 nm, most of which were micropores. However, the fiber existed in a non-crosslinked gel state, composed of microfibers as shown in the figure. During swelling in water, its spaces reached the level of a uniform macropore, and the internal diffusion rate became fast. Moreover, the diameter of the fiber was 10 microns, which is tens to one percent of the resin. The inner diffusion distance was short; hence the inner diffusion rate was very fast.

In addition, at very low ion concentration, the exchange rate was controlled by membrane diffusion. The membrane diffusion rate was mainly inversely proportional to the particle size, not only because the diameter of the fiber was small, but also because of the presence of microfibers, and the non-smooth surface reduced the diffusion film thickness, resulting in higher membrane diffusion rate. The concentration of surface charges also creates electrostatic attraction [47], which encourages the ions to move quickly. Amino phosphonic acid fibers are rich in negative electric groups around the surface and internal microfibers, which can further promote the movement of calcium and magnesium ions.

For the above reasons, amino phosphate fibers can quickly adsorb calcium and magnesium ions at very low or low concentrations, and this was confirmed by the experimental results, which showed that the amount of adsorption in the first 20 s reached more than 60% of the saturated adsorption amount. In addition, with the waning influence of the internal diffusion resistance, the adsorption rate became solely dependent on the chemical reaction rate, that is, the reaction rate was proportional to the products of the concentration of the target ions in the solution and the concentration of the unreacted functional groups, which is confirmed by the perfect fit of the adsorption rate to the pseudo-second-order reaction equation. In a nutshell, the superfast adsorption rate and high adsorption capacity of the fiber may be accounted for by the nano-tow networked structure formed inside the aminophosphonic acid chelating fiber and the uniform distribution of the effective functional groups on the surface of the nano-tow.

4. Conclusion

In order to meet the growing demand for the deep removal of Ca^{2+} and Mg^{2+} in the chlor-alkali industry, an aminophosphonic acid chelating fiber (PAN-PNa) was prepared from an amine-based fiber, PAN-PEI, by Kabachnik-Fields one-pot reaction with the existence of phosphorous acid and formaldehyde. The obtained PAN-PNa had a high adsorption capacity for Ca^{2+} and Mg^{2+} at low concentrations, and more importantly, it also exhibited a superfast adsorption rate, ensuring that its adsorption performance was fully achieved. Characterization of the fiber revealed that a nano-tow structure in the fiber which increased the effective adsorption area and shortened the diffusion path, may have been the main reason for the superfast adsorption rate of PAN-PNa for Ca^{2+}/Mg^{2+}. With the outstanding results of this study, PAN-PNa is expected to receive increased application for the deep purification of Ca^{2+} and Mg^{2+} in water in the chlor-alkali industry.

Conflict of interest

We declare that we do not have any commercial or associative interest that represents a conflict of interest in connection with the work submitted.

References

[1] J.-j. Wan, G.-l. Zhu, G.-x. Li, Y. He, Study on the technic of kai film brine refined, J. Salt Chem. Ind., 4 (2006) 1–3&9.
[2] Z. Ong, Y. Zhang, R. Cai, L. Wang, Q. Zhang, X. Huang, Study on Ca^{2+}, Mg^{2+} removal from salt type brine by NaOH and Na_2CO_3 for salt water production by nanofiltration, J. Salt Chem. Ind., 4 (2013) 17–19.
[3] H. Zhao, Operation essentials for calcium/magnesium ion adsorption by chelating resin, Guangzhou Chem. Ind., 13 (2011) 24–26.
[4] H. Li, Z. Zhang, H. Zhang, Y. Wang, X. Guo, B. He, The investigation of the production of refined brine used ln chloro-alkali membrane by D412 chelating resin ion, Exch. Adsorpt., 2 (1997) 195–202.
[5] D.H. Shin, Y.G. Ko, U.S. Choi, W.N. Kim, Design of high efficiency chelate fibers with an amine group to remove heavy metal ions and pH-related FTIR analysis, Ind. Eng. Chem. Res., 9 (2004) 2060–2066.
[6] C.A. Fetscher, S. Hills, S.A. Lipowski, N.J. Livingston, Process for conversion of amidoxime polymers to polyhydroxamic acids using aqueous hydrochloric acid solutions, Patente Americana, 3 (1967) 345–344.
[7] S. Kobayashi, M. Tokunoh, T. Saegusa, F. Mashio, Poly(allylamine). chelating properties and resins for uranium recovery from seawater, Macromolecules, 12 (1985) 2357–2361.
[8] S. Kobayashi, K.D. Suh, Y. Shirokura, Chelating ability of poly(vinylamine): effects of polyamine structure on chelation, Macromolecules, 5 (1989) 2363–2366.
[9] C.-C. Wang, C.-C. Wang, Adsorption characteristics of metal complexes by chelated copolymers with amino group, React. Funct. Polym., 66 (2006) 343–356.
[10] A.A. Shunkevich, Z.I. Akulich, G.V. Mediak, V.S. Soldatov, Acid–base properties of ion exchangers. III. Anion exchangers on the basis of polyacrylonitrile fiber, React. Funct. Polym., 63 (2005) 27–34.
[11] K. Tekin, L. Uzun, Ç.A. Şahin, S. Bektaş, A. Denizli, Preparation and characterization of composite cryogels containing imidazole group and use in heavy metal removal, React. Funct. Polym., 71 (2011) 985–993.
[12] E. Repo, L. Malinen, R. Koivula, R. Harjula, M. Sillanpää, Capture of Co(II) from its aqueous EDTA-chelate by DTPA-modified silica gel and chitosan, J. Hazard. Mater., 187 (2011) 122–132.
[13] Y. Xu, T. Wang, Z. He, M. Zhou, W. Yu, B. Shi, K. Huang, A polymerization-cutting strategy: self-protection synthesis of thiol-based nanoporous adsorbents for efficient mercury removal, Chemistry: A Eur. J., 24 (2018) 14436–14441.
[14] C.A. Fetscher, Extraction of Heavy of Metals from Solutions with Polyamidoximes, US,3088798[P].1963-05-07.

[15] I.L. Kalnin, A.H. di Edwardo, E.W. Choe, et al., Chemical Modification of Polyacrylonitrile Fiber for Carbonization, For NATL Meet of ACS 175th, California, 1978.
[16] G.S. Chauhan, S.C. Jaswal, M. Verma, Post functionalization of carboxymethylated starch and acrylonitrile based networks through amidoximation for use as ion sorbents, Carbohydr. Polym., 66 (2006) 435–443.
[17] I. Vega, W. Morris, N. D'Accorso, PAN chemical modification: synthesis and characterization of terpolymers with 1,2,4-oxadiazolic pendant groups, React. Funct. Polym., 12 (2006) 1609–l618.
[18] A.S. El-Khouly, Y. Takahashi, A.A. Saafan, E. Kenawy, Y.A. Hafiz, Study of heavy metal ion absorbance by amidoxime group introduced to cellulose-graft-polyacrylonitrile, J. Appl. Polym. Sci., 120 (2011) 866–873.
[19] M.F. Cheira, Characteristics of uranium recovery from phosphoric acid by an aminophosphonic resin and application to wet process phosphoric acid, Eur. J. Chem., 1 (2015) 48–56.
[20] M.C. Yebra-Biurrun, A. Bermejo-Barrera, M.P. Bermejo-Barrera, Synthesis and characterization of a poly(aminophosphonic acid) chelating resin, Anal. Chim. Acta, 1 (1992) 53–58.
[21] S.K. Sahni, R. Van Bennekom, J. Reedijk, A spectral study of transition-metal complexes on a chelating ion-exchange resin containing aminophosphonic acid groups, Polyhedron, 4 (1985) 1643–1658.
[22] Q. Ma, M. Lu, A new spherical aminophosphonic reins with phenolic backbone, Ion Exch. Adsorpt., 3 (2000) 239–246.
[23] Q. Pu, P. Liu, X. Wu, X. Chang, Z. Su, Synthesis and application of an aminophosphonic-carboxylic acid chelating resin for preconcentration of rare-earth elements, J. Lanzhou Univ. (Nat. Sci.), 3 (2002) 68–72.
[24] W. Dong, G. Zhang, J. Zhu, Preparation of amino chelating resins and these performances, Shanxi Univ. Sci. Technol., 2 (2010) 96–99&103.
[25] Z. Lu, Synthesis and Application of Aminophosphonic Acid Chelating Resin, Jiangnan University, 2008.
[26] Z. Shu, C. Xiong, X. Wang, Adsorption behavior and mechanism of amino methylene phosphonic acid resin for Ag(I), Trans. Nonferrous Met. Soc. China, 16 (2006) 700–704.
[27] Q. Xue, S. Xiao, C. Liu, J. Qiu, Preparation of α-aminophosphonates polymer gel and its adsorption of copper ion, Mater. Sci. Eng., 2 (2013) 131–134.
[28] R. Liu, H. Tang, B. Zhang, Removal of Cu(II), Zn(II), Cd(III) and Hg(II) from waste water by poly(acrylaminophosphonic)-type chelating fiber, Chemosphere, 13 (1999) 3169–3179.
[29] K. Vaaramaa, J. Lehto, H^+Na^+ exchange in an aminophosphonate-chelating, React. Funct. Polym., 33 (1997) 19–24.
[30] A.W. Trochimczuk, J. Jezierska, New amphoteric chelating/ion exchange resins with substituted carbamylethylenephosphonates; synthesis and EPR studies of their Cu(II) complexes, Polymer, 41 (2000) 3463–3470.
[31] Diamond Shamrock Corporation, Cation-Exchange Resins Having Cross-Linked Vinyl Aromatic Polymer Matrix with Attached Amino Alkylene Phosphonic Acid Groups, Their Use, and Preparation, US-4002564-A, 1977.01.11.
[32] E. Bayer, X.N. Liu, U. Tallarek, A. Ellwanger, K. Albert, M. Kutubuddin, Polystyrene-immobilized poly(ethylene imine) chains — a new class of graft copolymers, Polym. Bull., 37 (1996) 565–572.
[33] P.A. Riveros, The removal of antimony from copper electrolytes using amino-phosphonic resins: improving the elution of pentavalent antimony, Hydrometallurgy, 105 (2010) 110–114.
[34] J. Lehto, K. Vaaramaa, H. Leinonen, Ion exchange of zinc on an aminophosphonate-chelating resin, React. Funct. Polym., 33 (1997) 13–18.
[35] K. Moedritzer, R.R. Irani, The direct synthesis of α-aminomethylphosphonic acids. Mannich-type reactions with orthophosphorous acid, J. Org. Chem., 31 (1966) 1603–1607.
[36] The Dow Chemical Company, Process for Preparing an Aminonethylphosphonic Chelating Resin, EP0350172, 1993-06-23.
[37] International S.A. Duolite, M.A.G. Cornette, J. Carbonel, J.E.A. Franc, P.D.A. Grammont, Alkylaminophosphonic Chelating Resins, Their Preparation and Use in Purifying Brines, US 4818773,1989-4-4.
[38] S. Belfer, S. Binman, E. Korngold, Introduction of pyridine moeities into sulfochlorinated polyethylene hollow fibers, React. Polym., 25 (1995) 37–46.
[39] L. Dominguez, K.R. Benak, J. Economy, Design of high efficiency polymeric cation exchange fibers, Polym. Adv. Technol., 12 (2001) 197–205.
[40] W. Lin, Y. Lu, H. Zeng, Extraction of gold from Au(III) ion containing solution by a reactive fiber, J. Appl. Polym. Sci., 49 (1993) 1635–1638.
[41] R. Liu, H. Tang, B. Zhang, Adsorption characterization of aminophosphonic chelating fiber for Hg(II) ion, Environ. Chem., 3 (1998) 231–236.
[42] A. Jyo, Y. Hamabe, H. Matsuura, Y. Shibata, Y. Fujii, M. Tamada, A. Katakai, Preparation of bifunctional chelating fiber containing iminodi(methylphosphonate) and sulfonate and its performances in column-mode uptake of Cu(II) and Zn(II), React. Funct. Polym., 70 (2010) 508–515.
[43] Y. Bai, Z. Chen, B. Liu, G. Huang, Structural properties characterization and preparation of crosslinking carboxylic fibers based on polyacrylonitrile fibers, China Synth. Fiber Ind., 243 (2019) 41.
[44] B. Meng, Z. Chen, G. Huang, D. Liu, Preparation of amine chelating fiber and its adsorption properties for Cu^{2+}, China Synth. Fiber Ind., 6 (2017) 28.
[45] Q. Fan, Adsorbent Preparation from Waste Molecular Sieve and Study of its Adsorption Behavior of Water Hardness, China University of Petroleum, China, 2012.
[46] J. Wang, Application of Fluorinated Amino Phosphonic Acid Chelating Resins in Refining of Secondary Brine for Ion-Exchange Membrane Electrolysis, Chlor-Alkali Ind., 12 (2010) 12–16.
[47] Y. Liu, X. Zhang, J. Wang, A critical review of various adsorbents for selective removal of nitrate from water: structure, performance and mechanism, Chemosphere, 291 (2022) 132728, doi: 10.1016/j.chemosphere.2021.132728.